IFE/KR/F-87/046

EVALUATION OF HYDROGEN PRODUCTION FROM CO_2 CORROSION OF STEEL DRUMS IN SFR PART 2

by Arne Dugstad

June 1987

	KJELLER	HALDEN
ADDRESS	N-2007 Kjeller, Norway	N-1751 Halden, Norway
TELEPHONE	+47 2 712560 - 713560	+47 31 83100
TELEX	74 573 energ n	76 335 energ n
TELEFAX	+47 2 715553	

AVAILABILITY

Open

REPORT TYPE

REPORT NO.
IFE/KR/F-87/046

DATE
June 30, 1987

REPORT TITLE
EVALUATION OF HYDROGEN PRODUCTION FROM CO_2 CORROSION OF STEEL DRUMS IN SFR, part 2.

DATE OF LAST REV.

REV. NO.

CLIENT
SKI, Stockholm

NUMBER OF PAGES
11

CLIENT REF.

SKI 13. 293/85 86058

NUMBER OF ISSUES
35

SUMMARY

An experimental program has been carried out for the investigation of the hydrogen formation due to corrosion of steel by water containing CO_2 produced by microbiologic decomposition of paper in waste drums. The hydrogen production will be limited by a limited rate of CO_2 production, as CO_2 is consumed by corrosive reactions producing carbonate containing corrosion products. Experiments indicated that also iron oxide and hydroxides were formed together with $FeCO_3$ at low CO_2 partial pressures but at a rate which leads to a rather slow increase in hydrogen production. Hydrogen evaluation has been overestimated in previous reports on this subject.

DISTRIBUTION

Stig Wingefors, SKI 30x
File 5x

SUMMARY

Directors
Project management, Halden
Section heads

KEYWORDS Nuclear waste, CO_2 corrosion, steel

	NAME	DATE	SIGNATURE
PREPARED BY	Arne Dugstad Ketil Videm	June 30, 1987	Arne Dugstad Ketil Videm
REVIEWED BY			
APPROVED BY			

TABLE OF CONTENTS

1. INTRODUCTION

It is referred to SKI's order 13.7-293. The project is addressed to some specific aspect of aqueous CO_2 corrosion of drums in the repository for reactor waste, SFR. The drums are supposed to be filled with either concrete water or ground water. The pH in this water is between 6 and 13 and will normally give a very low corrosion rate when the oxygen in the water is consumed. However, biological degradation of paper and organic substances in the waste will lead to CO_2 production. As water with CO_2 is corrosive to steel, the corrosion rate can increase and hence also the formation rate of H_2.

To predict corrosion rates offshore it is often referred to a formula worked out by DeWaard and Milliams /1/.

$$\log R = 7.96 - 2320/(t+273) - 5.55t/1000 + 0.67 \log P_{CO_2}$$

where R = corrosion rate in mm/year and P_{CO_2} is CO_2 partial pressure in bar. Calculations of corrosion rates at 5^0C and 25^0C as a function of CO_2 partial pressure are shown in Figure 1. The results are applicable in <u>pure water</u> with dissolved CO_2, pH will then be below 4.5. There is also a lower limit for the CO_2 pressure. At low CO_2 pressure the reduction of H^+ and H_2O will be the dominating mechanism, while DeWaard and Milliams' formula applies when reduction of carbonic acid is important. DeWaard and Milliams' /1/ formula applies for carbon steels without corrosion and cannot be used for corrosion with carbonate films. At high pH film formation will be stimulated.

Increase of pH decreases the corrosion rate. Experiments at IFE have shown a 2-3 times reduction in corrosion rate when pH is increased from four to five in the presence of CO_2.

Survey of literature, tests at IFE and thermodynamic calculation indicate that the corrosion film formed at high CO_2 pressure (>0.5 bar CO_2 partial pressure) consists mainly of $FeCO_3$. Formation of the $FeCO_3$

film consumes CO_2 at the same rate as the corrosion of the Fe (metal). As a consequence it is not possible to have a high corrosion rate and at the same time maintain a high CO_2 partial pressure in a system with limited CO_2 sources.

If $FeCO_3$ is the only solid corrosion product formed, the corrosion rate will be limited by the production rate of CO_2 gas. It is anticipated that 0.5 mol CO_2 is evolved per drum per year /2/. This gives a corrosion rate of $1.4*10^{-3}$ mm/ year /3/. According to DeWaard and Milliams' formula an equilibrium CO_2 partial pressure of 0.005 bar in pure CO_2 containing water will give this corrosion rate. However, DeWaard and Milliams' equation is out of its validity region and published results of the effect of pH on the corrosion of steel can not be used due to the too low, but still marked effect of the CO_2 production.

Thus, to predict the corrosion rate in the drums it is necessary to do experiments. Tests have therefore been performed at pH 4.5, 5.5, 6.0, 6.5, 8.5 and 9.0 at 0.1 bar CO_2 partial pressure and 0.02 bar CO_2 partial pressure. The composition of the corrosion films have been analysed with X-ray, ESCA and Auger to see whether CO_2 is consumed or not. Experiments with carbon steel electrically connected to twice the area of AISI 316 have teen performed to see the effect of galvanic coupling between stainless steel in the waste and the drums.

2. EXPERIMENTAL

2.1. Test equipment

The experiments were carried out in 2.0 l glass cells shown in Figure 2. The lids had Quickfit connections for pH electrode, specimen rack. CO_2 gas, flushing gas and a venting tube which also acted as the inlet for HCl and NaOH to adjust pH.

During the experiments CO_2 was continuously bubbled through the cell. At start up and under changing of specimens and electrodes the cell was thoroughly flushed with N_2 to avoid contamination of O_2. The experiments were performed at room temperature (25^0 C).

2.2. Materials

The specimens were made of St.52.3 (0.17% C, 0.48% Si, 1.33% Mn, 0.077% Cr, 0.016% P, 0.019% S). Two different geometries of the specimens were used:

1. Tubes mounted in a rack as shown in Figure 3. The tubular specimens were electrically insulated from each other and from the stainless steel rack with teflon.

   All the specimens had electrical connection through the tubular specimen rack to make possible potential and LPR measurements.

2. 15 flat test coupons mounted on a ring in the lower half of the glass cell. The ratio between the area of the 15 coupons and the volume of the cell correspond to the ratio between the inner area and the volume of the drum. The flat coupons had no electrical connection.

2.3. Measurement of the corrosion rate

The corrosion rate was measured with either weight loss coupons or electrochemically.

The linear polarization resistance was measured once a day in some of the tests. This technique is based on measuring the relationship of electrode potential to current close to the corrosion potential, typically $\pm$ 10mV. The change of potential ΔE, relative to the change of current Δi, gives the polarization resistance R_p (analogous to Ohms Law):

$\frac{\Delta E}{\Delta i} = R_p$. The corrosion current is then given by the simple relationship: $i_{corr} = \frac{B}{R_p}$ where B is a constant dependent on the type of metal or alloy used for the electrode probe and also on the environment. Based on previous work a polarization constant of 20 mV was used to calculate the corrosion rates. The exposures lasted either 14 days or 28 days.

2.4. Control of the corrosive environments

Critical aspects with respect to the control of the test environments are:

- Deoxygenation
- Control of CO_2 level
- Removal of corrosion products and impurities
- Control of pH.

Distilled water was deaerated by boiling overnight in stainless steel containers with a vent tube. This water was, in the hot condition, fed into the N_2 flushed glass cell. The different CO_2 levels 0.1 bar and 0.02 bar CO_2 pressure were achieved by bubbling at 1 bar pressure argon mixed with 10% CO_2 and 2% CO_2, respectively.

The pH was controlled daily and adjusted if necessary with small addition of either HCl or NaOH.

In some tests the corrosion products were continuously removed by ion exchanger. This is analogous to the environment in the drums just after the corrosion has started. In other tests the environment was saturated with Fe^{2+} by corroding steel wool before the specimens were locked into the cell. This is analogous to the "normal" situation in the drums where the water is saturated with respect to Fe^{2+}.

2.5. Surface analyses

The corroded specimens were examined with X-ray, Auger (AES) and ESCA (XPS). X-ray analyses were conducted in a Philips X-ray spectrometer at IFE. The Auger and ESCA (XPS) analyses were conducted in a Varian Automatic Auger microprobe and a Vacuum Generators ESCA Lab. II spectrometer at SINTEF, Trondheim. The analytic characteristics of ESCA (XPS) and AES techniques are compared in Table 1. As implied by this table, AES is particularly useful for obtaining rapid depth profiles of surface films, whereas ESCA can be used to obtain information on the nature of chemical bonding.

Four specimens were analysed with ESCA and Auger and a few more with only Auger. The specimens were surface analysed and depth profiles were obtained with the AES technique.

One of the specimens were corroded at high CO_2 partial pressure to guarantee that the corrosion film mainly consisted of $FeCO_3$. This film was used to identify the binding energy (BE) of the C(1s) peak and O(1s) peak in $FeCO_3$.

3. RESULTS

3.1. Corrosion rates

The results obtained are devided into two groups. Tests in environment with low Fe^{2+} concentration <3 ppm and test in environment saturated with Fe^{2+}. The corrosion rate as a function of pH is shown in Figures 4 and 5, respectively. Open points represent results from the weight loss coupons and black points from LPR measurements.

The corrosion rate decreased 2-4 times depending upon pH and CO_2 partial pressure when the Fe^{2+} concentration was increased from <3 ppm to saturation. The difference decreased with increasing pH and increasing CO_2 partial pressure.

The LPR measurements showed a decrease in the corrosion rate the first 24 hours and then a fairly constant rate was achieved. The polarization constant of 20 mV fits with the weight loss results up to pH about 6. Using the 20 mV constant at higher pH showed a too high corrosion rate and is not indicated in Figs. 4 and 5.

The potential was almost constant after 1 to 2 days' exposure. Table 3 shows the potential after 7 days' exposure under the different test conditions listed in Table 2. The potential difference at 0.1 bar and 0.02 bar CO_2 is less than 10 mV. In environment with low and high Fe^{2+} concentration the difference is greater than 80 mV.

In tests with twice the area of AISI 316 connected to the specimen, the potential increased 2-4 mV. This increase did not influence the corrosion rate.

3.2. Film formation

The specimens are uniformly corroded. No pits were detected. Corrosion films formed in Fe^{2+} saturated solutions between pH 4.5 and 6.5 were almost black and they were soft with poor adherence. Films formed at higher pH had better adherence and they could not be wiped off.

X-ray analyses showed no peaks apart from elemental Fe. The results indicate that the corrosion product is amorphous.

AES surface analyses showed no unexpected peaks. An example is shown in Fig. 7. Apart from the main peaks from iron, carbon and oxygen only small peaks of alloying elements were detected.

Fig. 8 is an AES depth profile of a specimen with a thick film exposed at 0.1 bar CO_2, pH 5.0 and 28 days (test No. 9). The significance of the depth profile is that the oxygen, iron and carbon peak intensity as a function of depth are nearly constant indicating a homogenous composition of the corrosion film.

The depth profiles of the thinnest films were difficult to interpret because the signal from the iron substrate was mixed with the signal from the iron in the corrosion film.

To separate between chemical shift, some of the specimens were analysed with ESCA. A C(1s) spectrum and an O(1s) spectrum are shown in Figures 9 and 10, respectively. Chemical shifts are seen in both spectra. The energies of the most important peaks and the relative intensity corrected for the variation in sensitivity of different elements are listed in Table 4. The difference in energy between the C(1s)-, O(1s)- and Fe(2p2/3) peaks from specimen 2 and specimen 1, 3 and 4, respectively, originate from small matrix shifts due to the mixing of oxide and carbonate in specimen 1, 3 and 4. The results show that the composition of the corrosion product from specimen 2 exposed at 0.1 bar CO_2 (test No. 9) is nearly 100% $FeCO_3$. The corrosion products from specimen 3 and 4 (0.02 bar CO_2 and pH 5.5 and 8.5, respectively) contained a mixture of $FeCO_3$ and oxide/hydroxide. Specimen 3 30% oxide and specimen 4 75% oxide/hydroxide. The accuracy of the quantitative analyses is roughly $\pm$ 10%.

4. DISCUSSION

4.1. Corrosion rates

The results show that the corrosion rate is dependent of the iron concentration, CO_2 partial pressure and strongly dependent of pH. The water in the drums is saturated with Fe^{2+} after a relatively short

time when pH is >6.5. The solubility of Fe^{2+} as a function of pH at 0.02 bar and 0.1 bar CO_2 partial pressure is shown in Fig. 6.

These data can be applied for the waste barrels. After an initial period dependent of the starting pH, the CO_2 pressure will reach the CO_2 level corresponding to steady state corrosion. At this level the consumption of CO_2 by corrosion and the production rate are equal. This CO_2 level can be estimated from the present results. The CO_2 production is stated to be 0.5 mol CO_2/barrel per year. If $FeCO_3$ is the only corrosion product formed, the corrosion rate of the steel in mm/year is obtained by applying the inner steel surface area of the drum, provided a uniform attack.

$$\text{corr rate} = \frac{\text{mol Fe corroded*mol weight}}{\text{time*drum area*steel density}} = 1.4*10^{-3} \text{ mm/y.}$$

However, ESCA and Auger study of the corrosion film show that oxides are formed together with carbonate at low CO_2 partial pressure. The results from the analyses of two of the films formed at pH 6.5 and pH 8.5, respectively, are discussed in more detail. The oxide represent 30% (70% carbonate) and 75% (25% carbonate) of the corrosion product. With a CO_2 production rate of 0.5 mol CO_2/drum year, 70% and 25% carbonate in the corrosion product correspond to a corrosion rate of $2*10^{-3}$ mm/year and $5-6*10^{-3}$ mm/year, respectively (100% carbonate corrsponds to $1.4*^{-3}$ mm/year).

The corrosion rate actually measured in the two experiments referred above is $3-4*10^{-2}$ mm/year (pH 6.5) and $5*10^{-3}$ mm/year (pH 8.5). The corrosion rates correspond to a consumption rate of CO_2 about 20 times the anticipated, CO_2 production rate for pH 6.5 and almost the same as the anticipated CO_2 production rate at pH 8.5. Thus, at pH 6.5 a CO_2 partial pressure of 0.02 bar can not be maintained due to the high consumption rate of CO_2. The equilibrium CO_2 partial pressure will, therefore, be lower.

Auger analysis of the specimen exposed to 0.005 bar CO_2 at pH 6.0 showed a mixture of carbonate and oxide. Thus, even at this low CO_2 partial pressure CO_2 is consumed. From the carbonate content in the corrosion film and the measured corrosion rate it can be concluded

that the equilibrium pressure likely will be below 0.005 bar in the SFR repository with the specified CO_2 production rate. Therefore, the corrosion rate may be even lower than that measured for 0.005 bar CO_2. The corrosion rate measured at 0.005 bar CO_2 was $2*10^{-2}$ mm/year.

At pH 8.5 and CO_2 partial pressure 0.02 bar the experiments showed that the consumption rate of CO_2 is almost equal to the production rate. The equilibrium pressure at steady state corrosion in these experiments are therefore about 0.02 bar and the maximum corrosion rate $5-6*10^{-3}$ mm/year.

In the discussion so far active corrosion is assumed. If the steel is passivated the CO_2 pressure will increase beyond the equilibrium pressure at active corrosion and sooner or later the corrosion starts again. At higher CO_2 pressure a higher carbonate content in the corrosion product is expected and the net corrosion rate averaged over time is believed to be equal or lower to the corrosion rate at steady state.

The experiments indicate that the corrosion rate at low CO_2 partial pressure is higher than the sum of the individual contributions from the direct reduction of H^+ and H_2O and from CO_2 corrosion alone. A synergic effect is seen and it is reasonable that CO_2 catalyses the reaction slightly, but the increase in corrosion rate is assumed to be without practical consequences.

These experiments show that the corrosion rates and hence also the hydrogen production rates will be much lower than stated in the report by Preece, Arup and Grönvold /4/. The corrosion rates will also be lower than suggested in the report by Dahl /5/.

Our thermodynamic calculation indicated that $FeCO_3$ should be the stable corrosion product for all exposure conditions considered /3/. From an evaluation of the corrosion mechanism we pointed at the possibility of the formation of oxide containing corrosion products, despite their lower thermodynamic stability. The present experiments indicate that this is the case for the lowest CO_2 partial pressure.

This means that a treatment of the hydrogen production based on the simple reaction

$$Fe + H_2O + CO_2 = FeCO_3 + H_2$$

where the CO_2 supply is limited, underestimated hydrogen production. For the experimental conditions studied the maximum error is a factor of four. However, the hydrogen production is nevertheless small.

The corrosion rates (10^{-3} to 10^{-2} mm/y) suggested by us previously on a basis of general kinetics of the types of reactions involved are in agreement with the prediction for the corrosion rates of the waste drums based on the present experiments at pH 6.5-7 and above. At lower pH our meaurements resulted in somewhat higher values, but likely an increased exposure period would reduce the corrosion rates.

We want also to mention that the detected presence of oxide in the corrosion films not fully proves that CO_2 corrosion of steel led to such films. Origins of the oxide could also be the very thin films formed in air prior to the exposure. Another possibility is that trace amounts of oxygen in the solution precipitated iron oxides of higher valency (which are less soluble than two valency) at the specimen surface. Additional experiments to get a better insight of this would be desirable.

5. CONCLUSIONS

- The experiments resulted in a steady state corrosion rate in the waste drums about or less than $2*10^{-2}$ mm/year at pH 6. The corrosion rate decreases with increasing pH and increases with decreasing pH.

- At 0.1 bar CO_2 partial pressure the corrosion film consisted solely of $FeCO_3$. At CO_2 partial pressure equal or lower than 0.02 bar oxides were also found although thermodynamic calculations (presented in the report IFE/KR/F-86/019) indicated that $FeCO_3$ should be the thermodynamically stable corrosion product.

- The report SFR-83-03 and SFR-81-09 greatly overestimate hydrogen production by applying a treatment for the corrosion rate of steel drums which hardly is applicable for the conditions in SFR and by not taking into account that the corrosion reactions consume carbon dioxide. A treatment with a high corrosion rate and a high CO_2 partial pressure at the same time is unrealistic.

- It is not fully proven that the oxide found on the coupons in these experiments originates from CO_2 corrosion. Therefore, may even the low corrosion rates predicted for the waste containers from the present experiments be somewhat too high.

6. REFERENCES

/1/ DeWaard, C., Milliams, D.E.: 1st International Conference on the internal and external protection of pipes. Durham, England, September 9-11, 1975, paper F1.

/2/ Technical Report SKI 84:2.

/3/ Dugstad, A., Videm, K.: Evaluation of hydrogen production from CO_2 corrosion of steel drums in SFR. IFE/KR/F-86/019.

/4/ C. M. Preece, H. Arup, F.O. Grönvold. SKBF/KBS SFR 81-09.

/5/ L. Dahl. SKBF/KBS SFR 83-03.

TABLE 1. ANALYTICAL CHARACTERISTICS OF ESCA AND AES

	ESCA	AES
Energy Range		
Kinetic energies (eV)	100-1500	50-2500
Escape depth (Å)	20	20
Peak location (eV)	± 0.1	± 1
Chemical information	Oxidation state Organic structure Bonding	Marginal
Elemental sensitivity		
Elements	Z>3	Z>3
Specificity	very good	good
Sensitivity variations	50X	50X
Quantitative analysis		
Absolute	± 10%	± 30%
Relative	± 5%	± 5%
Detection limit	0.1% monolayer	0.1% monolayer
Matrix effects	some	some
Other aspects		
Vacuum (torr)	10^{-5}-10^{-10}	10^{-8}-10^{-19}
Depth profiling	yes, slow	yes, rapid
X-Y resolution	Variable >50 μm	>0.05 μm
Speed	slow, typical run - 30 min	Fast, elemental mapping in minutes
Sample destruction	None in 95% of the samples	Frequent, severe in tne case of organic compounds

TABLE 2. SUMMARY OF RUN CONDITIONS AND RESULTS FOR TESTS CARRIED OUT IN THE PROJECT

Test	pH	$[Fe^{2+}]$	Duration days	pCO_2 bar	Corrosion rate mm/y Weight loss	LPR
1 1	4.5	partly	14	0.1	0.13	0.16
2		saturated			0.15	
1					0.12	
2 2	5.5	saturated	14	0.1	0.12	
3					0.12	
1					0.08	
3 2	6.5	saturated	14	0.1	0.09	
3					0.09	
1					0.006	
4 2	8.5	saturated	14	0.1	0.005	
3					0.007	
5 1	4.5	partly	14	0.02	0.10	0.09
2		saturated			0.11	
1					0.035	
6 2	6.5	saturated	14	0.02	0.04	
3					0.05	
7	8.5	saturated	14	0.02	0.005	
8	9.0	saturated	14	0.02	<0.003	
9	6.0	saturated	28	0.1	0.09	
10	7.0	saturated	28	0.1	0.07	
11	6.0	partly saturated	28	0.02	0.035	
12	7.0	saturated	28	0.02	0.03	
13 1	6.0	<3 ppm	14	0.1	0.25	
2					0.23	0.21
14 1	6.0	saturated	14	0.1	0.10	0.13
2					0.10	
15 1	6.0	<3 ppm	14	0.02	0.11	0.12
2					0.11	
16 1	6.0	partly	14	0.02	0.03	0.05
2		saturated			0.04	
17	4.5	<3 ppm	14	0.02	0.15	0.13
18	8.5	<1 ppm	14	0.02	0.007	
19	6.0	saturated	14	0.005	0.02	
20	4.5	<1 ppm	14	0.1	0.25	

TABLE 3. POTENTIAL AFTER 7 DAYS' EXPOSURE. REFERENCE ELECTRODE Ag/AgCl

		Fe^{2+} saturated	Fe^{2+} <3 ppm
Test 1	0.1 bar CO_2, pH 4.5	0.671 (Ag/AgCl)	
Test 2	0.1 bar CO_2, pH 5.5	0.700 (Ag/AgCl)	
Test 9	0.1 bar CO_2, pH 6.0	0.700 (Ag/AgCl)	
Test 13	0.1 bar CO_2, pH 6.0		0.745 (Ag/AgCl)
Test 3	0.1 bar CO_2, pH 6.5	0.708 (Ag/AgCl)	
Test 4	0.1 bar CO_2, pH 8.5	0.785 (Ag/AgCl)	
Test 5	0.02 bar CO_2, pH 4.5	0.675 (Ag/AgCl)	
Test 11	0.02 bar CO_2, pH 6.0	0.705 (Ag/AgCl)	
Test 15	0.02 bar CO_2, pH 6.0		0.765 (Ag/AgCl)
Test 6	0.02 bar CO_2, pH 6.5	0.714 (Ag/AgCl)	
Test 7	0.02 bar CO_2, pH 8.5	0.790 (Ag/AgCl)	
Test 8	0.02 bar CO_2, pH 9.0	0.805 (Ag/AgCl)	

TABLE 4. BINDING ENERGIES (IN eV) AND STOICH. COMPOSITION FOR SPECIES DETECTED IN THE CORROSION FILMS. ESCA RESULTS.

Specimen No.	Peak	B.E. ev	Stoich. comp.	Comments
Specimen 1	C(1s) carbonate	289.3	1.0	Reference
10 bar CO_2	O(1s) carbonate	531.8	5.7	containing
pH 5	O(1s) oxide	530.1	1.6	$FeCO_3$ and
	Fe(2p3/2) oxide/carbonate	711	1.7	iron oxides
Specimen 2	C(1s) carbonate	289.6	1.0	Nearly pure
0.1 bar CO_2	O(1s) carbonate	531.8	3.2	$FeCO_3$
pH 7	Fe(2p3/2) carbonate	710.3	1.0	
Specimen 3	C(1s) carbonate	289.2	1.0	Mainly $FeCO_3$
0.02 bar CO_2	O(1s) carbonate	531.4	4.1	with some
pH 6.5	O(1s) oxide	529.7	0.5	oxide or
	Fe(2p3/2) oxide/carbonate	710.6	1.5	hydroxide
Specimen 4	C(1s) carbonate	289.3	1.0	Mainly oxides
0.02 bar CO_2	O(1s) carbonate/hydroxide	531.5	10.8	and hydrox-
pH 8.5	O(1s) oxide	529.9	5.4	ides with
	Fe(2p3/2) oxide carbonate	710.9	4.3	some $FeCO_3$

$FeCO_3$ will have the stocih composition.

C(1s) carbonate	1.0
O(1s) carbonate	3.0
Fe(2p 3/2) carbonate	1.0
O(1s) oxide	0

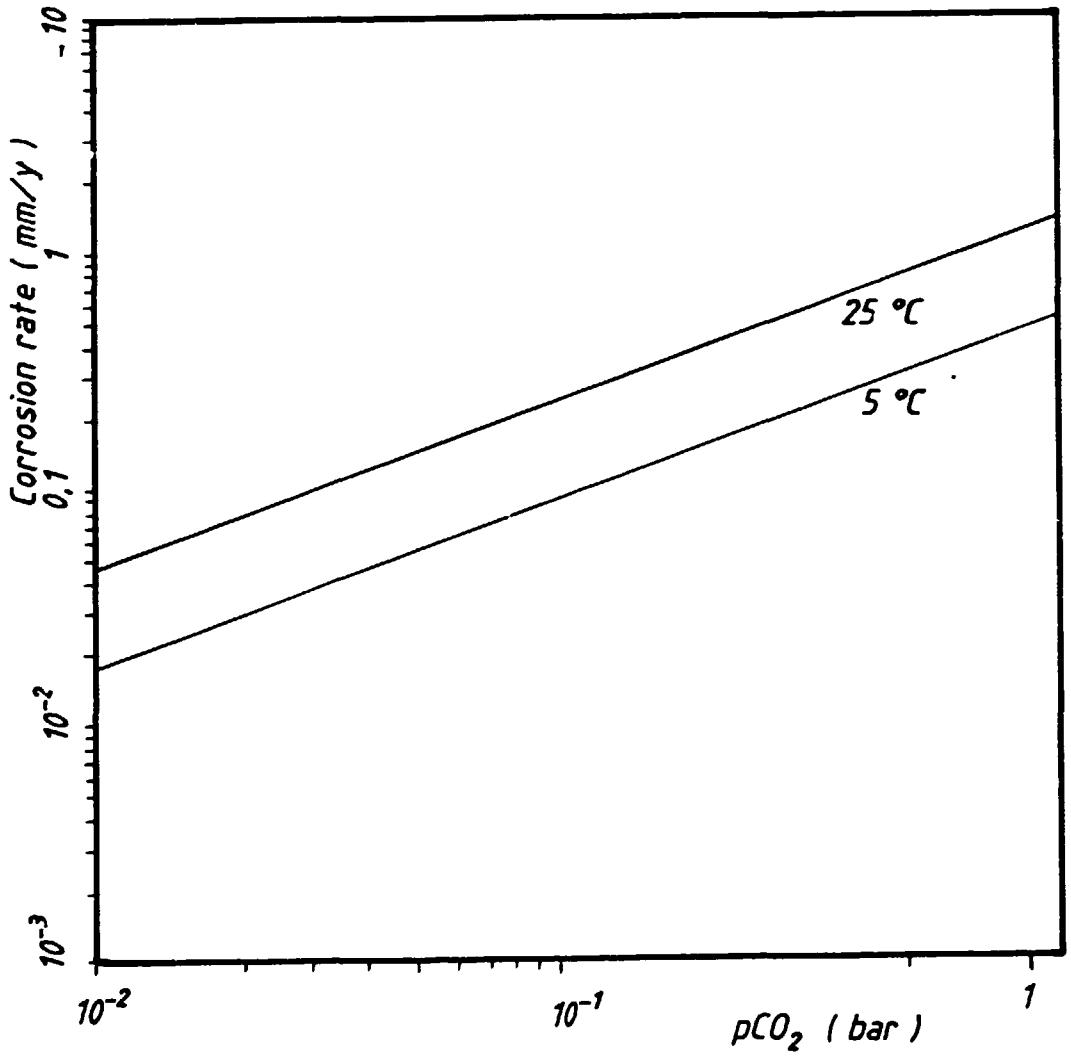

Fig. 1. Corrosion rate as a function of CO_2 partial pressure at 5^0C and 25^0C /1/

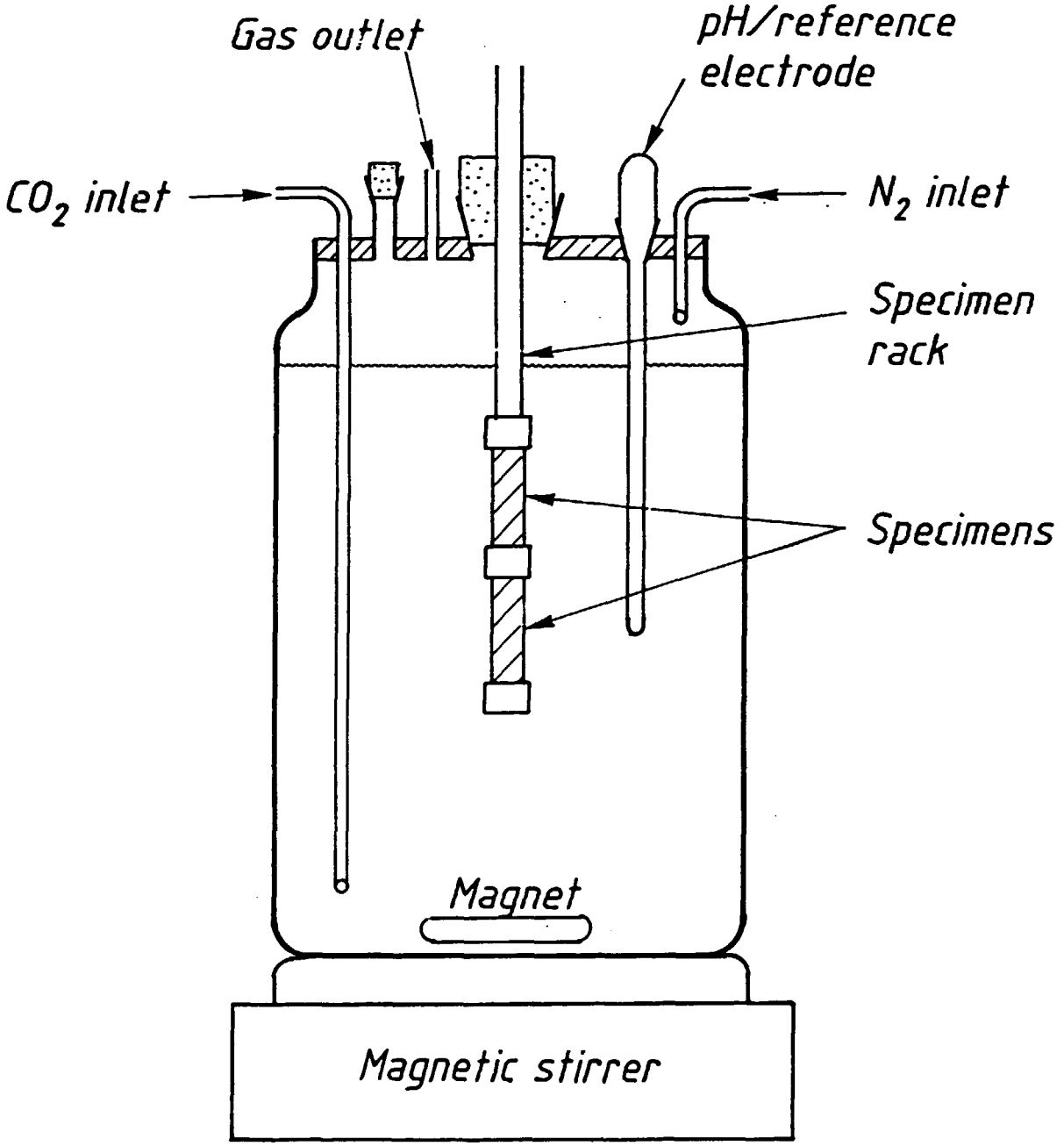

Fig. 2. Glass cell

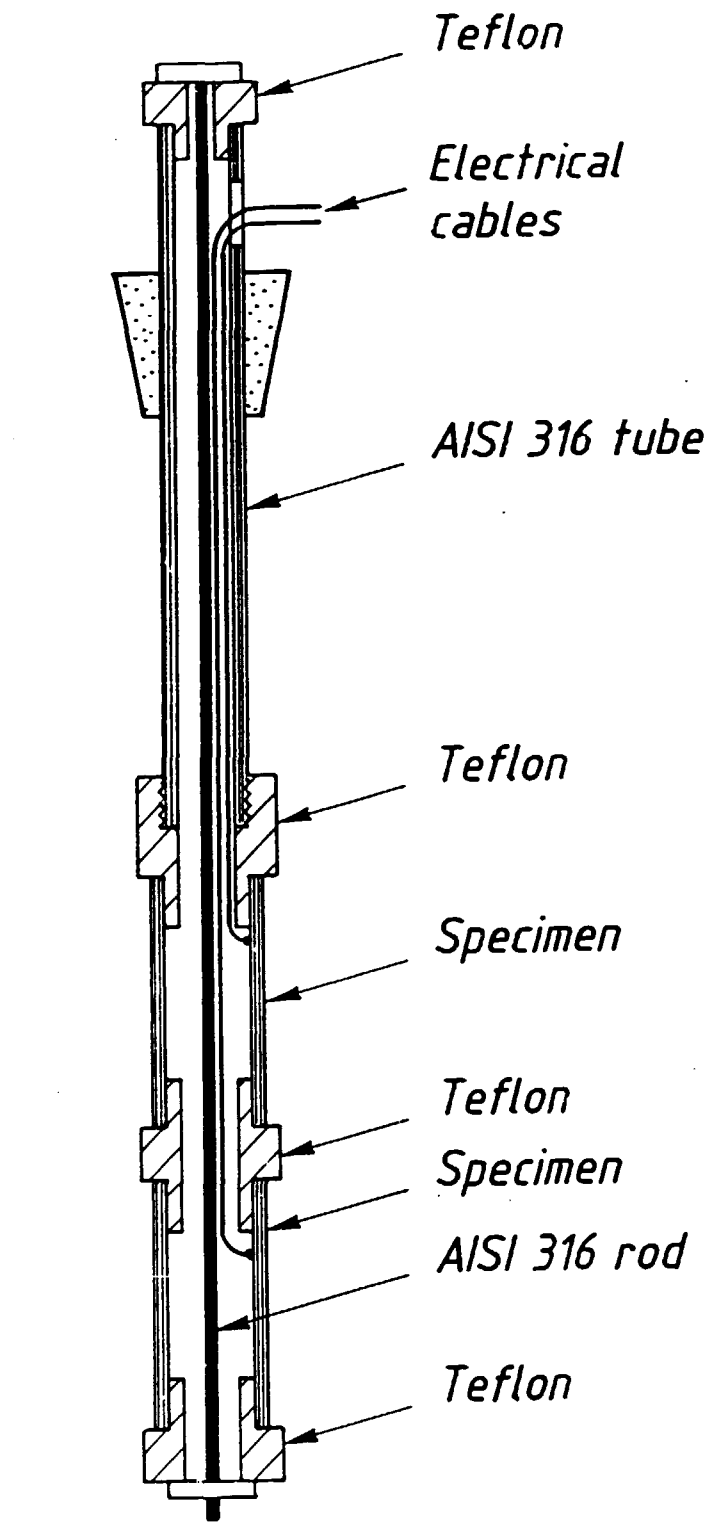

Fig. 3. Specimen rack with specimens

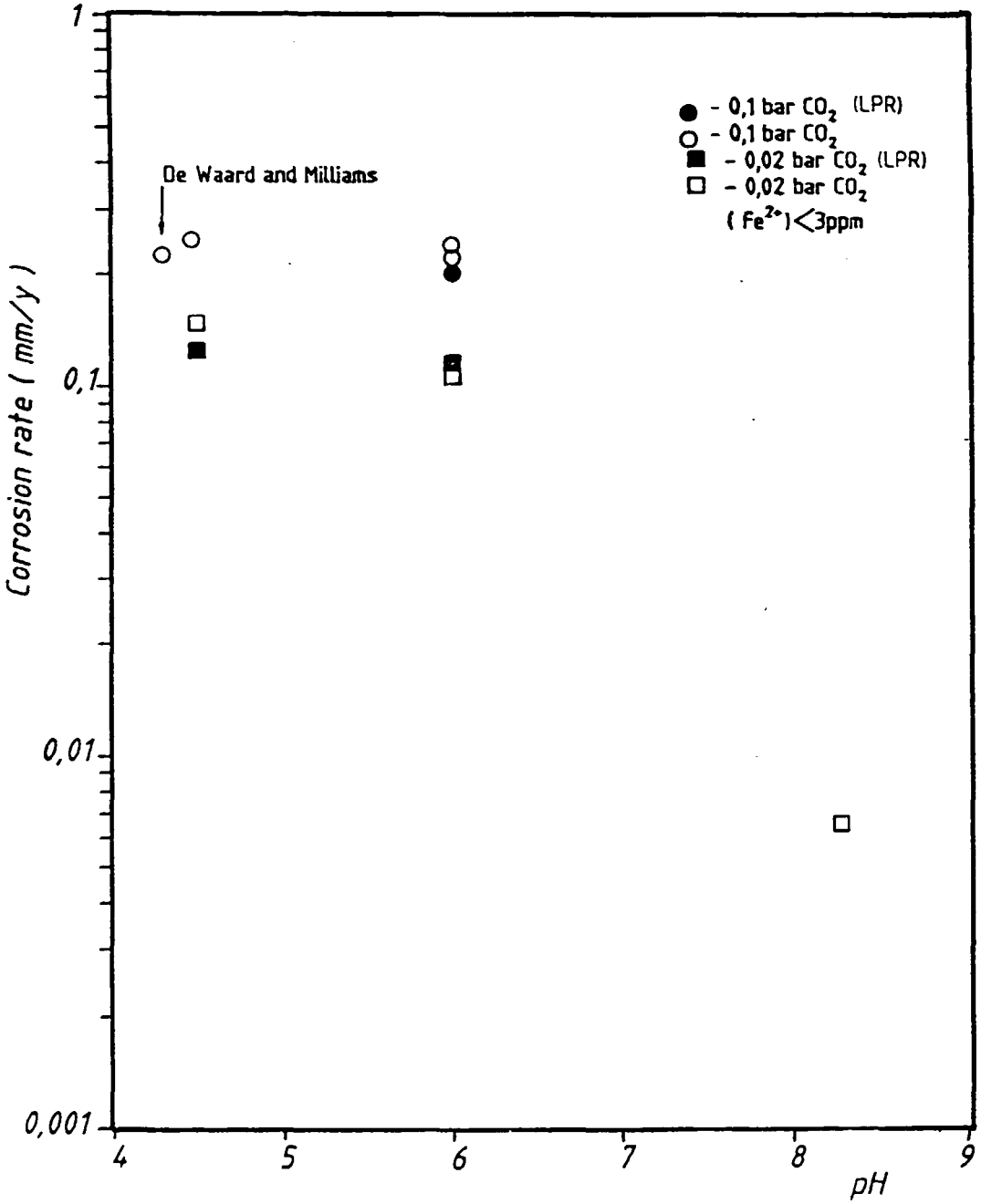

Fig. 4. Corrosion rate as a function of pH at 0.1 and 0.02 bar CO_2 partial pressure. The Fe^{2+} concentration is less than 3 ppm. See Table 2.

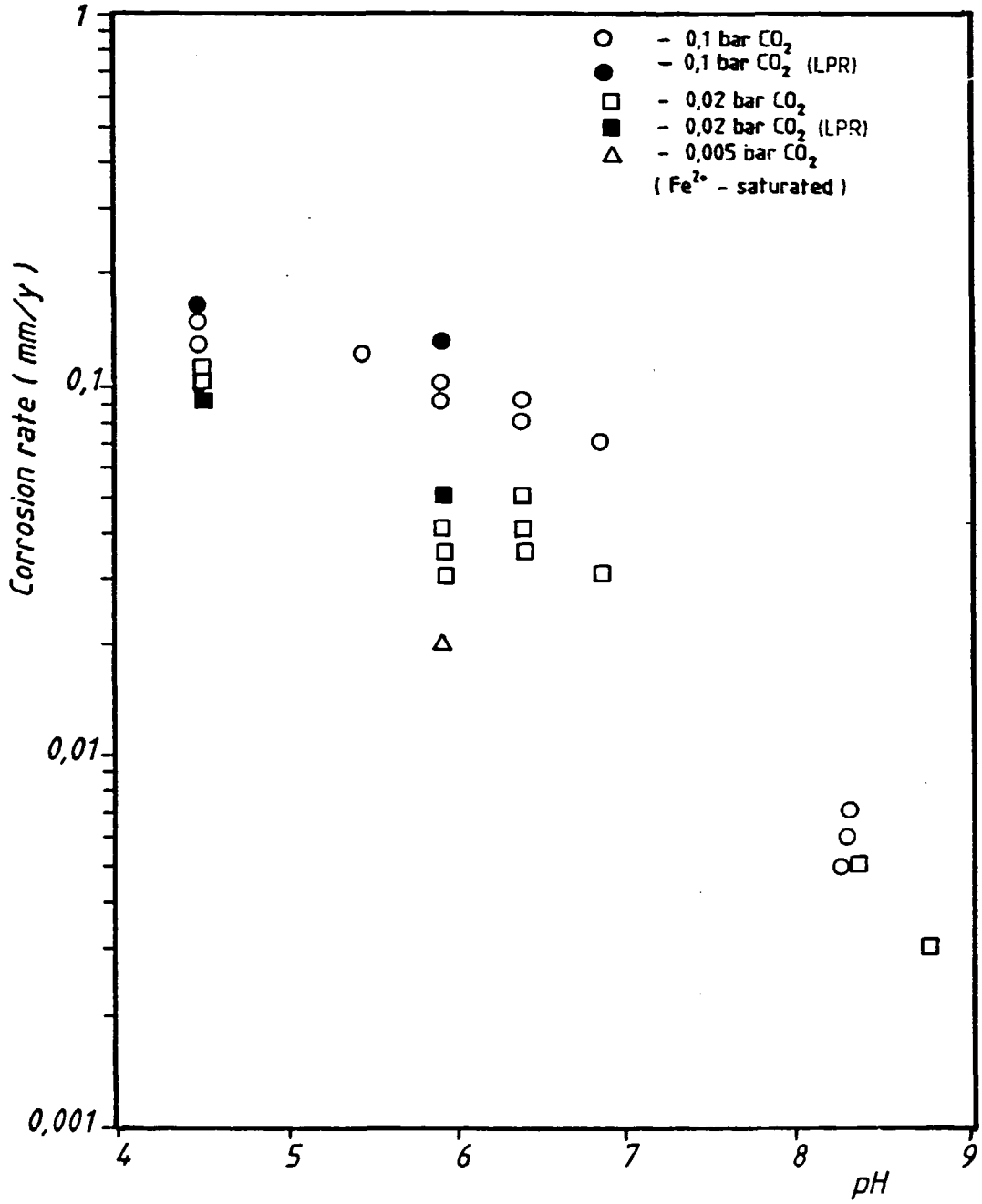

Fig. 5. Corrosion rate as a function of pH at 0.1 and 0.02 bar CO_2 partial pressure. The water is saturated or partly saturated with Fe^{2+}. See Table 2.

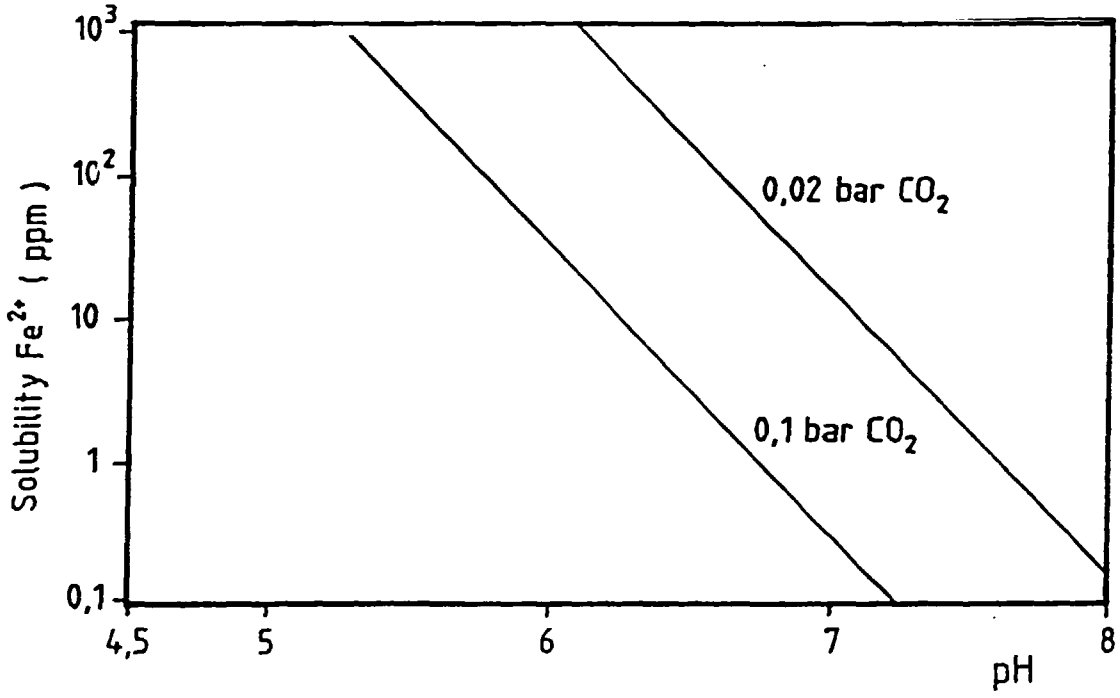

Fig. 6. Fe^{2+} solubility as a function of pH at 0.1 and 0.02 bar CO_2 partial pressure at 25°C.

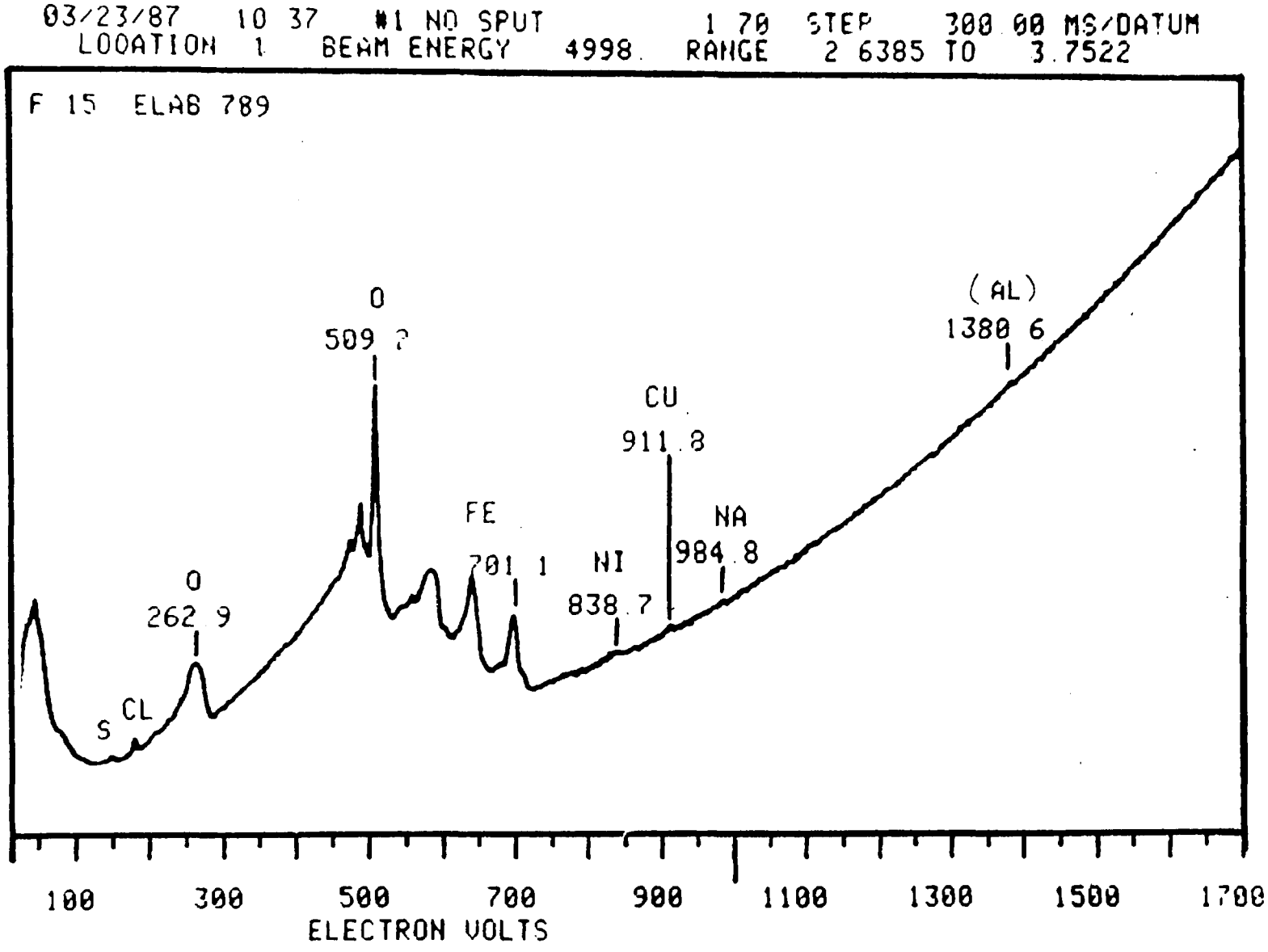

Fig. 7. AES surface analyses of a specimen after 28 days' exposure at 0.1 bar CO_2 and pH 6.0 (test No. 9).

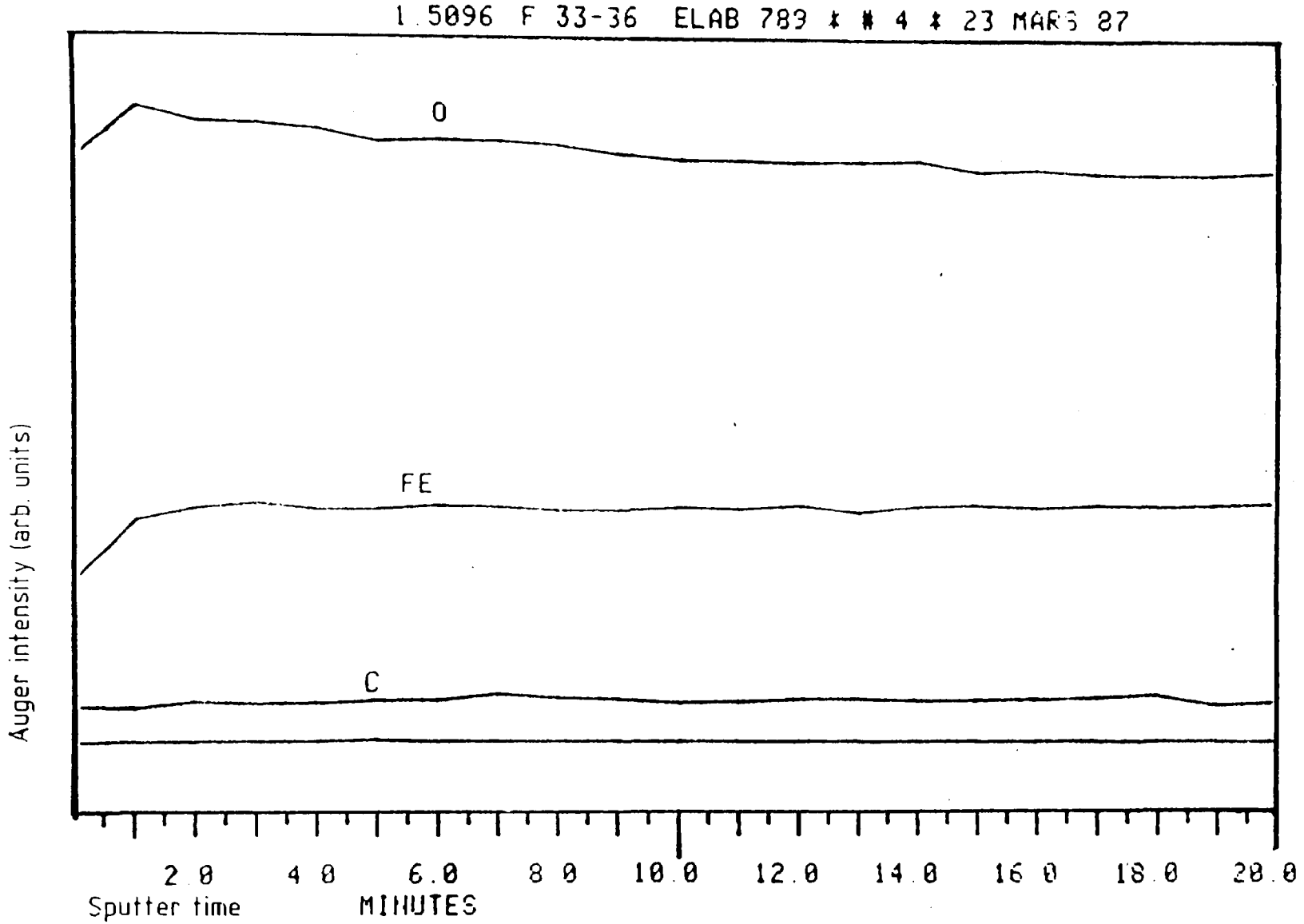

Fig. 8. AES depth profile of a specimen after 28 days' exposure at 0.1 bar CO_2 and pH 6.0 (test No. 9). The oxygen, iron and carbon peak intensity are shown as a function of depth. Depth is proportional to the sputter time.

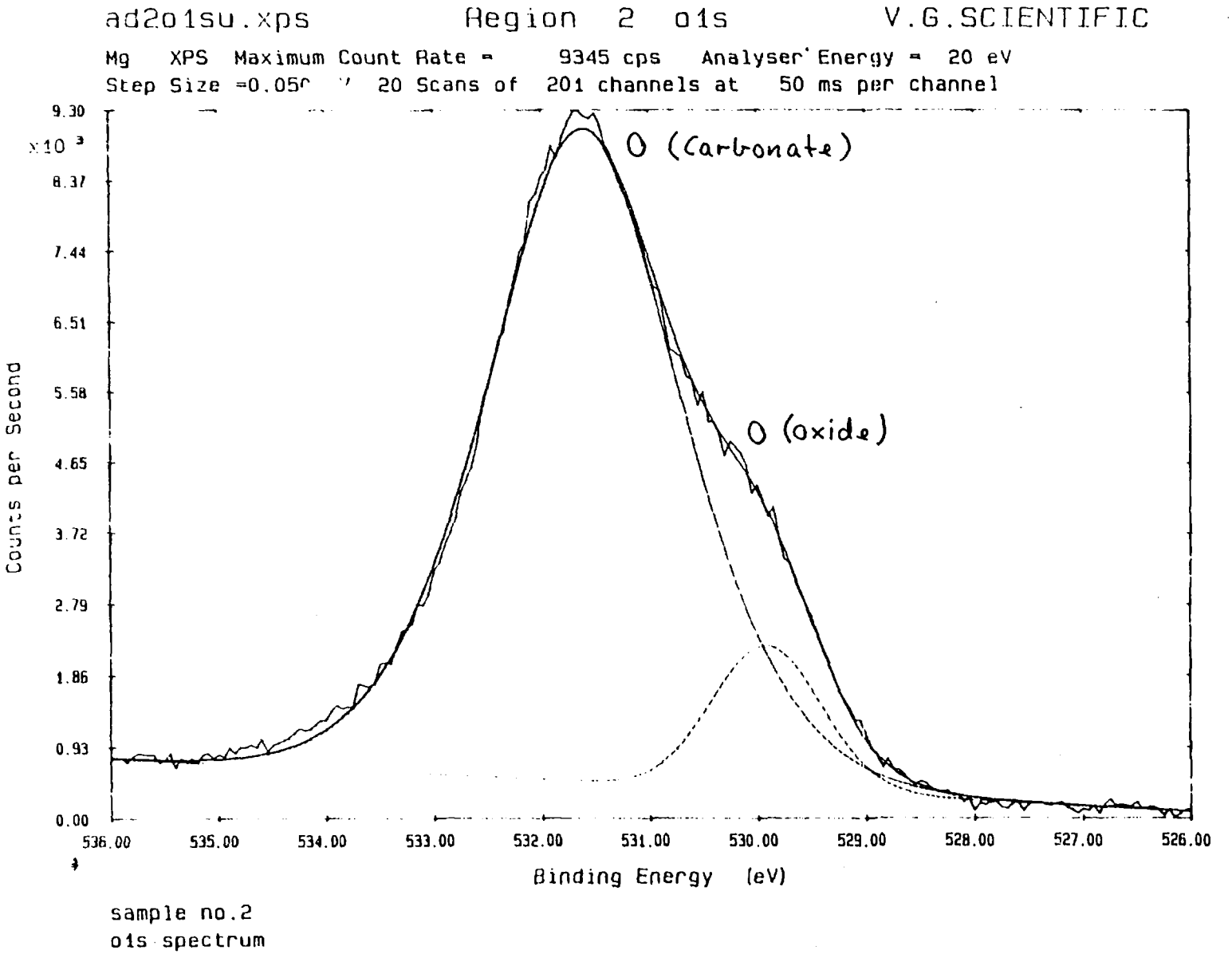

Fig. 9. Spectrum showing O(1s) peaks from oxygen in carbonate and oxygen in oxide.

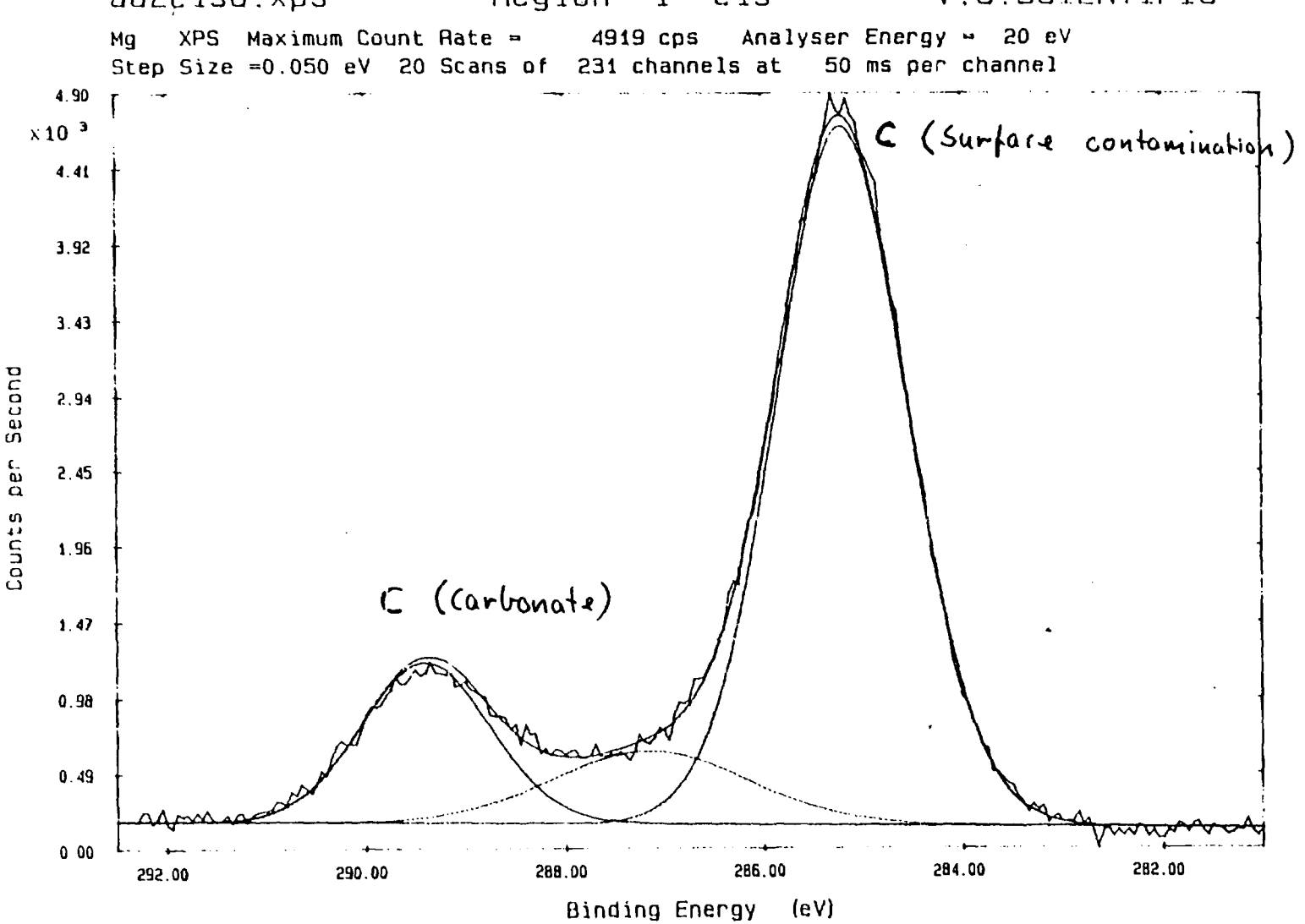

Fig. 10. Spectrum showing C(1s) peaks from carbon in carbonate and carbon from surface contamination.

Institutt for energiteknikk (IFE) ble grunnlagt i 1948 under navnet «Institutt for atomenergi». I 1953 ble Instituttet etablert som en uavhengig stiftelse. Hovedsentret ligger på Kjeller. Virksomheten i Halden er konsentrert om det internasjonale OECD Halden Reactor Project.
I 1980 ble Instituttets navn endret til «Institutt for energiteknikk». Idag er IFE med sine vel 500 ansatte et av de største teknologiske forskningsinstitutter i Norge.

AKTIVITETSOMRÅDER

- *PETROLEUMSTEKNOLOGI*
- *KJERNEKRAFT*
- *PROSESSTEKNOLOGI*
- *ENERGISYSTEMER/ENOK*
- *ISOTOPTEKNOLOGI*
- *MATERIALTEKNOLOGI*
- *GRUNNFORSKNING I FYSIKK*

FAGLIGE SPESIALITETER

- *NUKLEÆR BRENSELSTEKNOLOGI*
- *PROSESSKONTROLL*
- *INDUSTRIELL MATEMATIKK*
- *RESERVOARMODELLERING*
- *PETROLEUMSGEOLOGI*
- *FLERFASE TRANSPORT*
- *GASSTEKNOLOGI*
- *OLJEKORROSJON*
- *AVANSERTE SVEISEMETODER*
- *RADIOFARMAKA*
- *BESTRÅLINGSTEKNIKK*
- *STRÅLINGSTEKNISKE INSTRUMENTER*
- *FYSIKALSK-KJEMISKE ANALYSER*
- *FASTSTOFF FYSIKK*

Institutt for energiteknikk

Postboks 40, 2007 Kjeller
Tlf.: (02) 71 25 60
Telefax: (02) 71 55 53
Teleks: 74 573 energ n

Postboks 173, 1751 Halden
Tlf.: (031) 83 100
Telefax: (031) 83 103
Teleks: 76 335 energ n

Institute for energy technology (IFE) was founded in 1948 under the name of «Institutt for atomenergi». In 1953 the Institute was established as an independent foundation. The main center is located at Kjeller. The activity in Halden is concentrated on the international OECD Halden Reactor Project.
In 1980 the name was changed to «Institute for energy technology».
At present, IFE, with more than 500 employees, is one of the major technological research institutes in Norway.

MAIN ACTIVITIES

- *PETROLEUM TECHNOLOGY*
- *NUCLEAR POWER*
- *PROCESS TECHNOLOGY*
- *ENERGY SYSTEMS AND - CONSERVATION*
- *ISOTOPE TECHNOLOGY*
- *MATERIALS TECHNOLOGY*
- *BASIC RESEARCH IN PHYSICS*

SPECIAL ACTIVITIES

- *NUCLEAR FUEL TECHNOLOGY*
- *PROCESS CONTROL*
- *INDUSTRIAL MATHEMATICS*
- *RESERVOIR MODELLING*
- *PETROLEUM GEOLOGY*
- *MULTI-PHASE FLOW*
- *GAS TECHNOLOGY*
- *OIL CORROSION*
- *ADVANCED WELDING TECHNIQUES*
- *RADIOACTIVE PHARMACEUTICALS*
- *IRRADIATION TECHNIQUES*
- *RADIATION INSTRUMENTS*
- *PHYSICAL - CHEMICAL ANALYSES*
- *SOLID STATE PHYSICS*

Institute for energy technology

Box 40, N-2007 Kjeller, Norway
Teleph: +47 2 71 25 60
Telefax: +47 2 71 55 53
Telex: 74 573 energ n

Box 173, N-1751 Halden, Norway
Teleph: +47 31 83 100
Telefax: +47 31 83 103
Telex: 76 335 energ n